SERBIAN JOURNAL OF ELECTRICAL ENGINEERING
Vol. 15, No. 2, June 2018, 145-163

UDC: 519.87:[621.352.6+621.316.722.1 DOI: https://doi.org/10.2298/SJEE170822001S

Optimal Design of Controllers for Power Network Connected SOFC Using of Multi-objective PSO

Amin Safari[1], Hossein Shahsavari[1], Farshad Babaei[1]

Abstract: In this paper, we study the concept and forming manner of Solid Oxide Fuel Cell (SOFC) into the electrical system and then, its effect on small signal stability is investigated. The paper illustrates the essential module, mathematical analysis and small signal modeling of the SOFC joined to single machine system. The aim of this study is to reduce power oscillations in the presence of the SOFC with optimal stabilizer. The multi-objective Particle Swarm Optimization (MOPSO) technique has been used for designing a Power System Stabilizer (PSS) in order to improve the performance of the system. Two objective functions are regarded for the design of PSS parameters in order to maximize the damping factor and the damping ratio of the system. To evaluate the efficiency of the proposed optimal stabilizers, four scenarios are considered and then, its results have been analyzed. The proposed PSS tuning technique can be applied to a multi-machine system connected to the SOFC. The efficiency of MOPSO based proposed PSS on the oscillations the system related to SOFC is illustrated by time-domain simulation and also, the comparison of the MOPSO based proposed PSS with the PSS based-single objective method has been prepared.

Keywords: Solid Oxide Fuel Cell, Multi-objective PSO, Small Signal Model, Multi-machine System.

1 Introduction

An important issue in recent years, fuel cell (FC) study and expansion have received much attention due to their higher energy conversion efficiency and lower greenhouse gas emissions than other device in the processes of converting fuel into operational energies. One of the highest types of FC is Solid Oxide Fuel Cell (SOFC). Previous works that are performed for the SOFC power generations and have already been reported [1 – 3]. The SOFC with higher capacity can be regarded as a resource power generation in transmission network [4, 5]. Thus, the effect of the SOFC on small signal stability is important and should be investigated carefully [6 – 10]. Many studies are implemented on the SOFC power plant for the stability analysis of the

[1]Department of Electrical Engineering, Azarbaijan Shahid Madani University, Tabriz, Iran;
E-mail: safari@azaruniv.ac.ir

distribution system. For example, Das and Co-workers in [11] represented a dynamic model of the SOFC in the distribution system that works in island mode and in the grid joined mode. Ref. [12] illustrates a model for the SOFC stack that operates at relatively low pressures. Dynamic models of micro-turbine and FC as distributed generators and analysis its effect on the dynamic behavior of the system is introduced in [13]. This paper investigates that when the influence of FC generation achieves to the level of conventional generation in a power system, how the system small-signal stability is affected. Ref. [14] shows a decreased order dynamic model of gird-joined a FC power generation. In [15], the result of the SOFC model with the single machine system on the dynamic stability is checked. A complementary control signal in the excitation system provides fast damping of the oscillations and thus, dynamic performance is improved. Power system stabilizer (PSS) has been extensively used to repress the low frequency oscillations and improve the system dynamic stability. The present paper recommends a new technique for PSS design by using the multi-objective PSO to optimize the operation of the system. As regards, that optimization algorithms are being developed every day, but are still used algorithm PSO [16]. In this paper, the MOPSO is used in order for optimal design of PSS parameters for improving the performance of the system. Consequently, evaluation results of the MOPSO based planned controller, and then its good performance for damping of low frequency fluctuations under dissimilar disturbances are shown. The aims of this paper are:

- An accurate dynamic model of the SOF has been expanded to study transient stability in electrical systems;
- The proposed model devitalizes or even eliminates electromechanical oscillations;
- The MOPSO is exploited to obtain the optimal design of classic PSS parameters and PID parameters, in the existence of SOFC joined to the system.

The next sections of the paper are as follows. In Section 2, all of the electrical system components that are used for small signal stability research are presented. Section 3 shows the optimal method for scheming dissimilar PSS for a power system related to the SOFC. Section 4 contains solution method and analysis of time-domain simulation results of proposed optimization model and consequently, conclusions are given in Section 5.

2 Problem Model

This paper studies effect of adding SOFC to the power system on the electro-mechanical oscillation modes of the system. For PSS design, all of the power system components, e.g. generators, their control systems and the SOFC power plant must be first modeled. The MOPSO technique designs the optimal

stabilizers for improving the small signal stability by using the eigenvalues and deviation factors of the system.

2.1 SOFC model

The SOFC dynamic model is shown in Fig. 1.

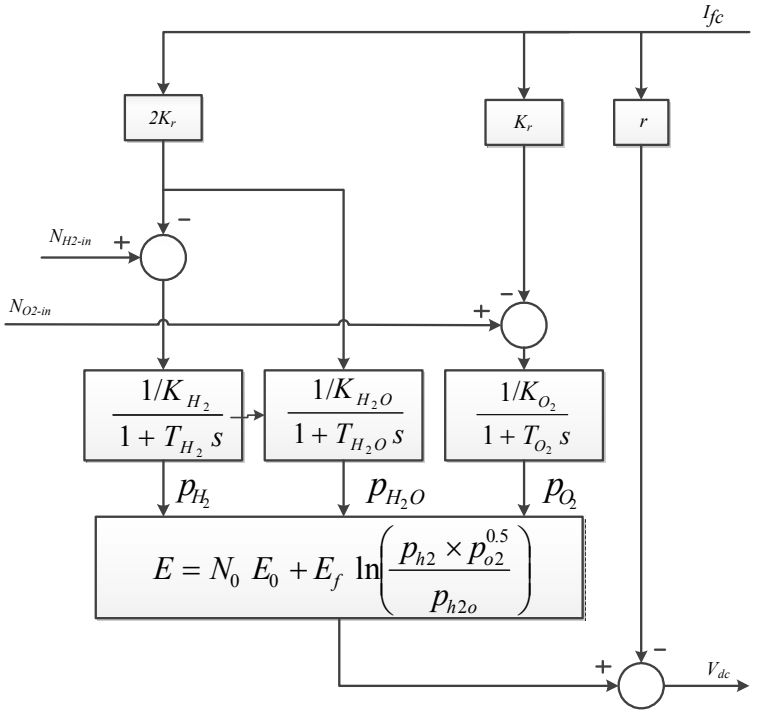

Fig. 1 – *SOFC dynamic model.*

The chemical reactions that are happening inside the cell for the production of electricity can be calculated as [6 – 10]:

$$\text{Anode: } H_2 + O^{=} \rightarrow H_2O + 2e^{-}, \tag{1}$$

$$\text{Cathode: } \frac{O_2}{2} + 2e^{-} \rightarrow O^{=}. \tag{2}$$

The SOFC output power should be in control of its output current, because SOFC power depends on its current. Therefore, we have:

$$I_{fc-ref} = \frac{P_{fc-ref}}{V_{fc}}, \tag{3}$$

where I_{fc-ref} is limited by the following boundaries, to ensure that SOFC is worked on the safe operating area [17]:

$$I_{fc-ref\max} = \frac{U_{\max}}{2K_r} q_{h2-in}, \tag{4}$$

$$I_{fc-ref\min} = \frac{U_{\min}}{2K_r} q_{h2-in} \quad K_r = \frac{N_0}{4F}, \tag{5}$$

where $U_{\max}$ and $U_{\min}$ are the maximum and minimum fuel unitization, respectively. The N_0 is the number of cells in series in the FC stack, q_{h2-in} is the hydrogen input flow rate, and *F* is the Faraday constant.

As regards the Nernst equation, the internal electromotive force of the FC stack can be calculated as:

$$E = N_0 E_0 + E_f \ln\left(\frac{p_{h2} \times p_{o2}^{0.5}}{p_{h2o}}\right), \quad E_f = \frac{N_0 RT}{2F}, \tag{6}$$

where E_0 is the voltage related to the reaction-free energy of a cell, *T* is the SOFC operating temperature, *R* is the gas constant, p_{h2}, p_{o2}, p_{h2o}, T_{h2}, T_{o2} and T_{h2o} are the reactant partial pressures and time constant of hydrogen, oxygen and water, respectively. Based on the dynamic model shown in Fig. 1, the U_{opt} is the optimal fuel utilization, T_f is the time constant of dynamic of fuel supply, r_{ho} is the ratio of hydrogen to oxygen, K_{h2}, K_{o2} and K_{h2o} are the valve molar constant for hydrogen, oxygen and water.

In order to analyze the small signal stability of a synchronous generator, small signal model is usually used. The synchronous generator model is well defined in a state space structure which is given in [18, 19].

2.2 SOFC model in single machine system

Fig. 2 shows the structure of the SOFC power generation joined to the single machine system. Equivalent reactance of transformers or/and transmission line is denoted by $x_s, x_{sb_1}, x_{sb_2}, x_{ts}$. Data information of a case study are given in Appendix. A DC-DC boost converter is exploited when SOFC output voltage is low for connecting to grid. Hence, we have:

$$d = d_0 + T_d\left(I_{fc-ref} - I_{fc}\right), \tag{7}$$

where *d* is the duty cycle and T_d is the transfer function of the FC current controller.

Fig. 3 shows the state space method to a DC-DC boost converterin continuous conduction mode (CCM). The boost converter has two states. First, the switch is on, second, the switch is off.

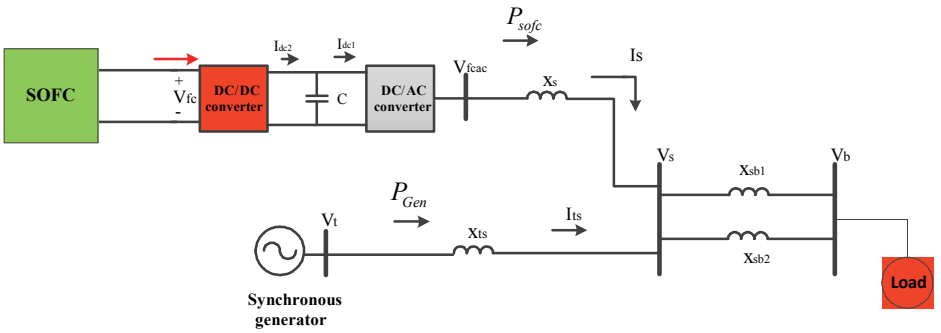

Fig. 2 – *Formation of the SOFC power generation connected to single machine system.*

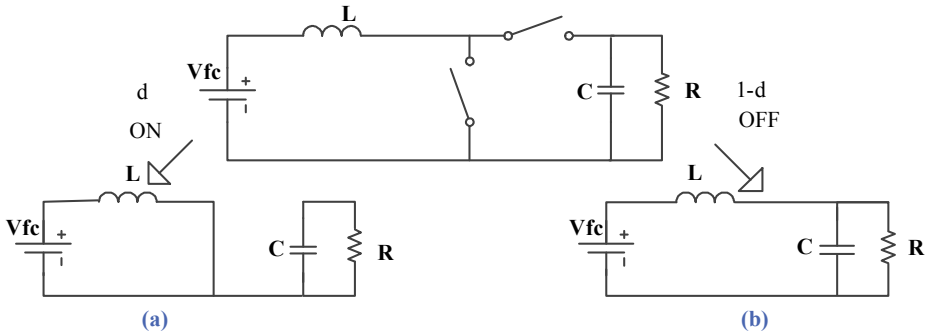

Fig. 3 – *Operating of DC-DC converter in two stages of switching.*

State space models for Figs. 3a and 3b can be expressed as follows, respectively:

$$\begin{aligned} \dot{x} &= A_{on}x + B_{on}u, \\ y &= C_{on}x + D_{on}u, \end{aligned} \tag{8}$$

$$\begin{aligned} \dot{x} &= A_{off}x + B_{off}u, \\ y &= C_{off}x + D_{off}u. \end{aligned} \tag{9}$$

These can be approximated by the following state space averaged model:

$$\begin{aligned} \dot{X} &= AX + Bu, \\ Y &= CX + Du, \end{aligned} \tag{10}$$

$$\begin{aligned} A &= dA_{on} + (1-d)A_{off}, \qquad C = dC_{on} + (1-d)C_{off}, \\ B &= dB_{on} + (1-d)B_{off}, \qquad D = DA_{on} + (1-d)D_{off}. \end{aligned} \tag{11}$$

Therefore,

$$\dot{i_L} = \frac{V_c \times d}{L} - \frac{V_C}{L} + \frac{V_{fc}}{L}, \tag{12}$$

$$\dot{V_C} = \frac{i_L}{C} - \frac{d \times i_L}{C} - \frac{V_C}{RC}, \tag{13}$$

where i_L is the DC-DC inductor current and V_c is the DC-DC capacitor voltage.

The changed DC voltage is converted to AC voltage by using a DC-DC converter for connecting to the power system. The terminal AC voltage of the converter can be calculated as follows [20]:

$$\overline{V}_{fcac} = mkV_{dc}\left(\cos\psi + \mathrm{j}\sin\psi\right), \tag{14}$$

where V_{dc} is the terminal voltage of DC-DC converter, ψ is the angle deviation between V_{fcac} and V_{dc} and k is usually equal to 0.75 [20]. Two different controllers are proposed for the DC-AC converter, where m is the modulation ratio and φ is the phase of the pulse width modulation:

$$\varphi = \varphi_0 + T_{vdc}(s)\left(V_{dc} - V_{dc-ref}\right), \tag{15}$$

$$m = m_0 + T_{vac}(s)\left(V_s - V_{s-ref}\right), \tag{16}$$

where T_{vdc} is transfer function of the DC voltage controller and T_{vac} is transfer function AC voltage controller. From Fig. 3 mathematical model of the DC-AC converter can be stated as:

$$\dot{V}_{dc} = \frac{1}{C_{dc}}\left(I_{dc2} - I_{dc1}\right). \tag{17}$$

We can have:

$$\overline{V}_t = \mathrm{j}x_{ts}\overline{I}_{ts} + \overline{V}_s, \tag{18}$$

$$\overline{V}_s = -\mathrm{j}(x_s)\overline{I}_s + \overline{V}_{fcac}, \tag{19}$$

$$\overline{V}_s - \overline{V}_b = \mathrm{j}x_{sb}\left(\overline{I}_{ts} + \overline{I}_s\right), \quad x_{sb} = x_{sb1} \,||\, x_{sb2}. \tag{20}$$

The equations are transferred to d-q frame of the synchronous machine. Hence, we have:

$$\begin{bmatrix} x_{sb} & x_s + x_{sb} \\ x_q + x_{ts} + x_{sb} & x_{sb} \end{bmatrix}\begin{bmatrix} i_{tsq} \\ i_{sq} \end{bmatrix} = \begin{bmatrix} -V_{fcac}\cos\psi + V_b\sin\delta \\ V_b\sin\delta \end{bmatrix}, \tag{21}$$

$$\begin{bmatrix} x_{sb} & x_s + x_{sb} \\ x_d^{'} + x_{ts} + x_{sb} & x_{sb} \end{bmatrix}\begin{bmatrix} i_{tsd} \\ i_{sd} \end{bmatrix} = \begin{bmatrix} V_{fcac}\sin\psi - V_b\cos\delta \\ E_q^{'} - V_b\cos\delta \end{bmatrix}. \tag{22}$$

2.4 Linearized Model

Linearization of a dynamic model of the DC-DC converter (12) and (13) can be found the following:

$$\Delta \dot{i}_{fc} = \frac{V_{fcac0}}{L}\Delta d + \frac{(d_0 - 1)}{L}\Delta V_c + \frac{1}{L}\Delta V_{fc}, \tag{23}$$

$$\Delta \dot{V}_c = -\frac{i_{fc0}}{C}\Delta d + \frac{(1 - d_0)}{C}\Delta V_c - \frac{1}{RC}\Delta V_{fc}, \tag{24}$$

$$\Delta \dot{d} = -T_1 \Delta \dot{i}_{fc} - T_2 \Delta i_{fc}. \tag{25}$$

For DC-AC converter, we have:

$$\Delta \dot{V}_{dc} = \frac{1}{C_{dc}}\left(\Delta I_{dc2} - \Delta I_{dc1}\right), \tag{26}$$

$$\Delta \varphi = T_{vdc}(s)\Delta V_{dc}. \tag{27}$$

$$\Delta m = -T_{vac}(s)\Delta V_s. \tag{28}$$

Linearized of (21) and (22) is denoted by the following:

$$\begin{bmatrix} \Delta i_{tsd} & \Delta i_{tsq} \end{bmatrix}^T = Q \begin{bmatrix} \Delta\delta & \Delta E_q^{'} & \Delta V_{dc} & \Delta m & \Delta\psi \end{bmatrix}^T, \tag{29}$$

$$\begin{bmatrix} \Delta i_{sd} & \Delta i_{sq} \end{bmatrix}^T = W \begin{bmatrix} \Delta\delta & \Delta E_q^{'} & \Delta V_{dc} & \Delta m & \Delta\psi \end{bmatrix}^T, \tag{30}$$

where

$$Q = \begin{bmatrix} Q_{11} & Q_{12} & Q_{13} & Q_{14} & Q_{15} \\ Q_{21} & Q_{22} & Q_{23} & Q_{24} & Q_{25} \end{bmatrix} \text{ and } W = \begin{bmatrix} W_{11} & W_{12} & W_{13} & W_{14} & W_{15} \\ W_{21} & W_{22} & W_{23} & W_{24} & W_{25} \end{bmatrix}. \tag{31}$$

Linearized SOFC can be written as:

$$\Delta I_{fc-ref} = -\frac{P_{fc-ref}}{V_{fc0}^2}\Delta V_{fc}, \tag{32}$$

$$\Delta I_{fc} = \frac{1}{1 + T_e s}\Delta I_{fc-ref}, \tag{33}$$

$$\Delta q_{o2-in} = \frac{1}{r_{ho}}\Delta q_{h2-in}, \tag{34}$$

$$\Delta q_{h2-in} = \frac{2K_r}{U_{opt}}\frac{1}{1 + T_f s}\Delta I_{fc-ref}, \tag{35}$$

$$\Delta p_{h2} = \frac{1}{K_{h2}} \frac{1}{1+T_{h2}s} \left(\Delta q_{h2-in} - 2K_r \Delta I_{fc} \right), \tag{36}$$

$$\Delta p_{o2} = \frac{1}{K_{o2}} \frac{1}{1+T_{o2}s} \left(\Delta q_{o2-in} - K_r \Delta I_{fc} \right), \tag{37}$$

$$\Delta p_{h2o} = \frac{1}{K_{h2o}} \frac{1}{1+T_{h2o}s} 2K_r \Delta I_{fc}, \tag{38}$$

$$\Delta V_{fc} = a_1 \Delta p_{h2} + a_2 \Delta p_{o2} + a_3 \Delta p_{h2o} + a_4 \Delta I_{fc}, \tag{39}$$

$$\Delta P_t = K_1 \Delta\delta + K_2 \Delta E_q^{'} + K_{pdc} \Delta V_{dc} + K_{pm} \Delta m + K_{p\psi} \Delta\Psi, \tag{40}$$

$$\Delta E_q = K_4 \Delta\delta + K_3 \Delta E_q^{'} + K_{qdc} \Delta V_{dc} + K_{qm} \Delta m + K_{q\psi} \Delta\Psi, \tag{41}$$

$$\Delta V_t = K_5 \Delta\delta + K_6 \Delta E_q^{'} + K_{vdc} \Delta V_{dc} + K_{vm} \Delta m + K_{v\psi} \Delta\Psi. \tag{42}$$

The block diagram of the system by using of the (27), (28), (32 – 38) and linearized equations that is given in [18, 19] is shown in Fig. 4.

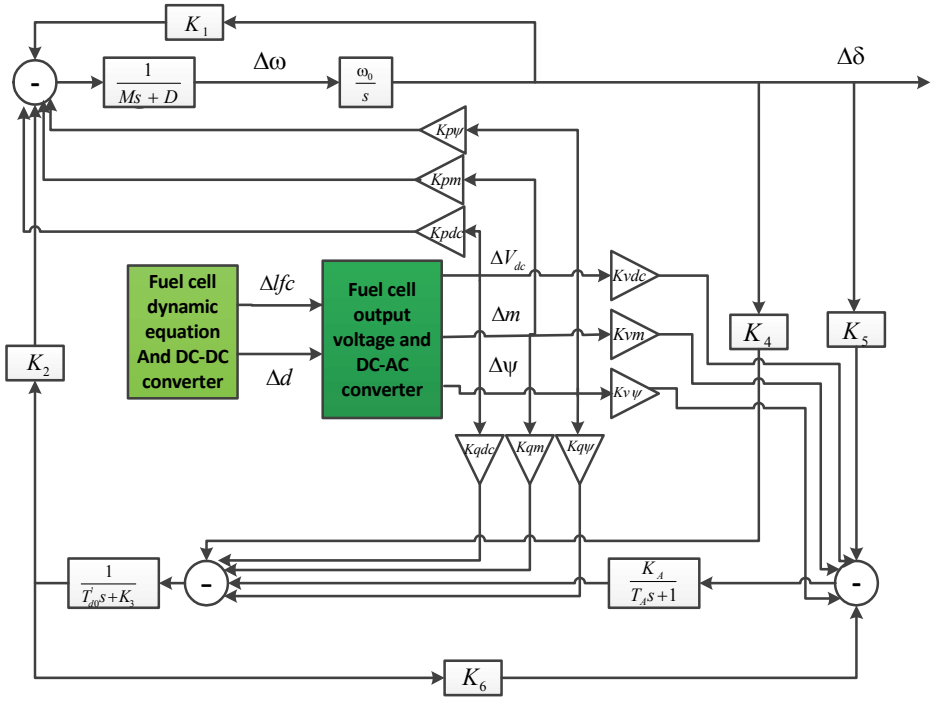

Fig. 4 – *Linearized model of the SOFC in single machine system.*

3 Solution Method

3.1 Multi-Objective Particle Swarm Optimization

The comparison of PSO with other heuristic algorithms makes the obvious concept under consideration a Pareto set ranking procedure [21] could be the straight way to develop the scheme to exploit the multi-objective optimization problems. The historical notation of optimum candidates obtained by a particle (i.e., an individual) could be handled to keep non-dominated candidates generated in the previous iterations. By using of global attraction strategies under consideration a historical notation found non-dominated candidates would put through convergence characteristic into globally non-dominated solutions. The optimization problem is a multi-objective optimization which was considered as an effective approach to find the optimal solution between different objectives. The detailed procedures for finding the best solutions by optimal Pareto set are introduced in Fig. 5.

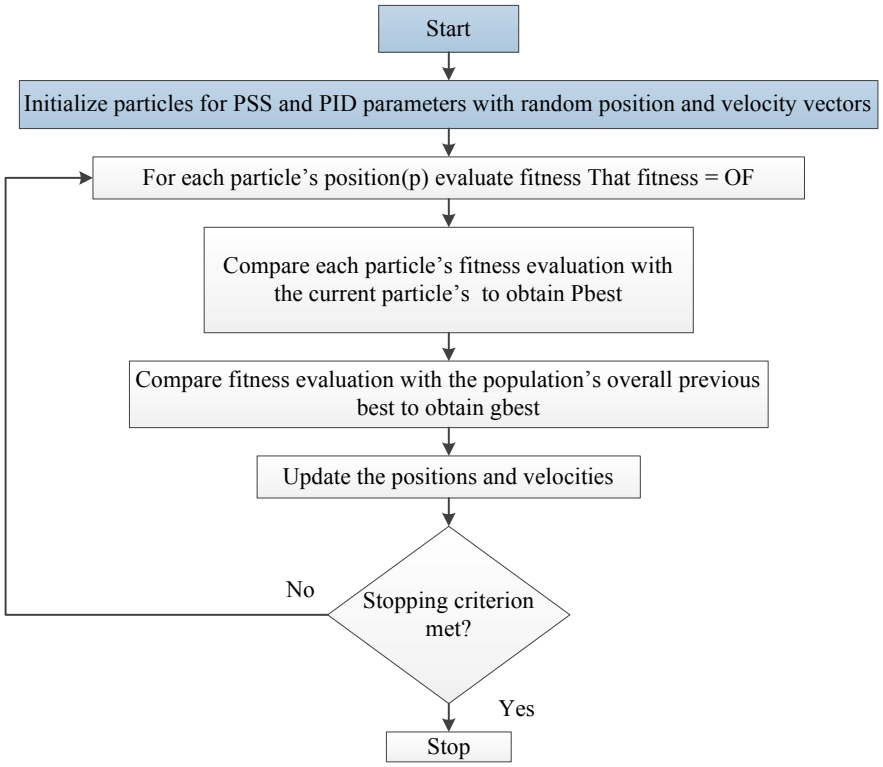

Fig. 5 – *A flowchart of MOPSO.*

3.2 Classic power system stabilizer

Fig. 6 illustrates model of the CPSS. The CPSS consists of two phase-lead compensation blocks, and a gain block. Five constant coefficients of the model (i.e. T_1, T_2, T_3, T_4, K_C) have to be designed optimally.

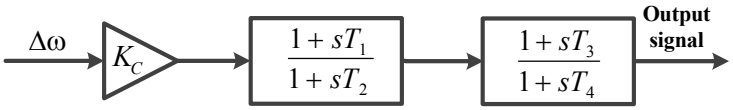

Fig. 6 – *The classic power system stabilizer.*

3.3 PID controller

The considered controller structure is PID controller, which is shown in Fig.7.

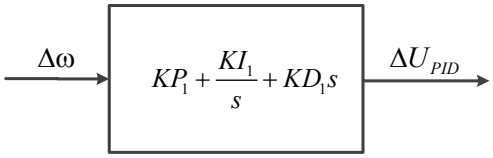

Fig. 7 – *PID controller.*

The PID is installed to synchronous generator. The parameters of PID controller $KI_{1,2}$ $KD_{1,2}$ $KP_{1,2}$ should be tuned by optimization algorithm.

4 Applying MOPSO Algorithm to Design the Optimal Controllers for SOFC

In the linearized system model presented, the eigenvalues of the single machine system are evaluated. The proposed method is aiming to search for the optimal parameters set of the controllers. The objective functions for MOPSO to tuning of controllers are defined by the following:

$$\begin{aligned} F_1 &= \sum_{j=1}^{n} (1-\xi_j), \\ F_2 &= abs(\Delta\omega) + OS, \\ OS &= \frac{r-y}{r} \times 100, \end{aligned} \tag{43}$$

where $\Delta\omega$ is the speed deviation of generator, OS is the system overshoot, n is the total number of the eigenvalues, ξ_j is the damping ratio, r is the system

reference, and y is the system output. The goal of these objective functions is to improve the damping of the oscillation and reducing the system overshoot and settling time. To have a comparison with MOPSO, single objective PSO is employed. This comparison helps us to have a better analyzes. The goal is minimization of the following fitness function:

$$OF = W_1 \times F_1 + W_2 \times F_2 , \tag{44}$$

where F_1 and F_2 are objective functions described already, W_1 and W_2 is the weighting ratios.

4.1 Optimal tune of inverter PID controller

The objective of the optimization problem is to maximize the damped oscillation due to imported disturbance. The best solution that obtained from MOPSO and PSO is summarized in **Table 1**.

Table 1
The optimal values of PID controller by using MOPSO and PSO.

Parameters	KI_1	KD_1	KP_1
Optimal value by MOPSO	-6.016	-0.59	3
Optimal value by PSO	0.795	0.193	-1.25

4.2 Optimal tuning of classic PSS

In this section, the parameters of the exciter (K_A, T_A) and PSS (T_1, T_2, T_3, T_4, K_c) should be tuned with the PSO and MOPSO. The input and output of the PSS are the speed deviation $\Delta\omega$ and the excitation voltage, respectively. The best solution obtained from MOPSO and PSO is given in **Table 2**.

Table 2
The optimal values of PSS and exciter parameters by using of MOPSO and PSO methods.

Parameters	T_1	T_2	T_3	T_4	K_C	T_A	K_A
Optimal value with MOPSO	1.1	0.13	1.02	0.21	1	0.1	9
Optimal value with PSO	2.03	0.07	1.68	0.70	1.15	0.17	9.38

5 Simulation Results

To analyze the small signal modeling of the SOFC joined to single machine system and proposed stabilizers, four scenarios will be considered. In these

scenarios assumed that $P_{SOFC} = 0.5$ and $P_{Gen} = 0.5$. The simulation of the system is tested by a mechanical torque entered into the generator. Fig. 8 shows the speed deviation of a single machine system without a controller that the system is unstable after high oscillations. Therefore, the SOFC power generation can makes instability in the system. To demonstrate the robustness of the MOPSO in tune of PSS, a multi-machine test system connected to SOFC is simulated.

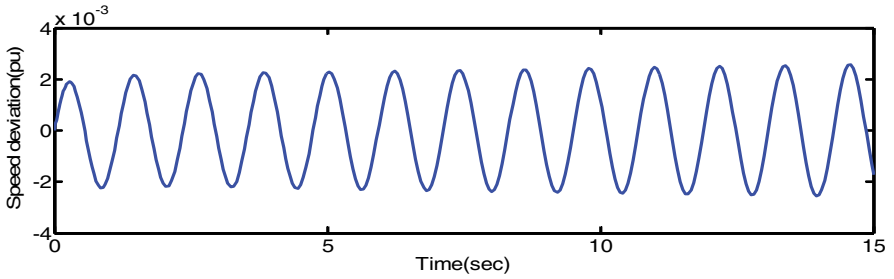

Fig. 8 – *Output signal of SOFC connected to SMIB system without controllers.*

5.1 A single machine connected to the SOFC

5.1.1 Scenario 1

In this scenario, generator is equipped with a classic PSS controller that tuned by single objective PSO. The convergence rate of the PSO is shown in Fig. 9a. So, it seems that the objective has a clear conflict here. Fig. 10 shows the plot of speed deviation response of the equipped generator with different stabilizers under the electromechanical disturbance. Fig. 11 shows the DC voltage deviation of output DC-DC converter with different controllers. The DC voltage deviation with regulated classic PSS and regulated PID is nearly the same.

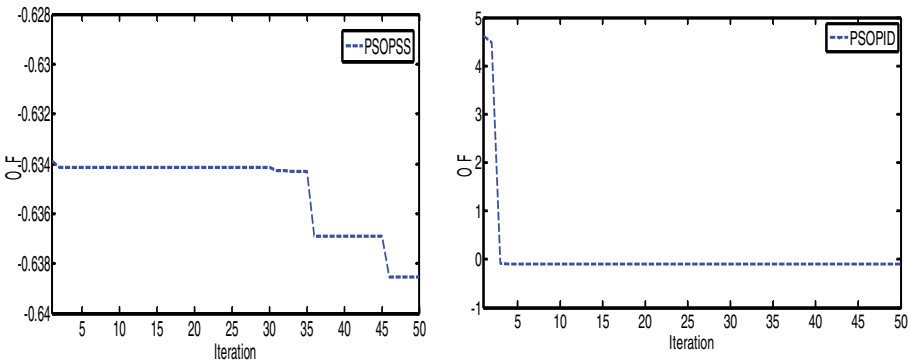

(a) (b)

Fig. 9 – *The convergence rate of the PSO in scenarios 1 and 2.*

4.1.2 Scenario 2

In this scenario, generator is equipped with PID controller that tuned by single objective PSO. The convergence rate of the PSO is shown in Figs. 9b. So, it seems that the objective have not very clear conflict here. The speed deviation of the system with different controllers in this scenario is shown in Fig. 10. By visual inspection of the curves in Fig. 10, it can be seen that the speed deviation of the system equipped with classic PSS reached a better damping against PID controller. Although, the speed deviation with tuned PID controller reached a relatively good damping. It is noticed that the speed deviation with PSO based classic PSS is better than that with PSO based PID with less settling time and overshoot. The DC voltage deviation of output DC-DC converter with different controller is shown in Fig. 11, which demonstrates that the CPSS has a better response.

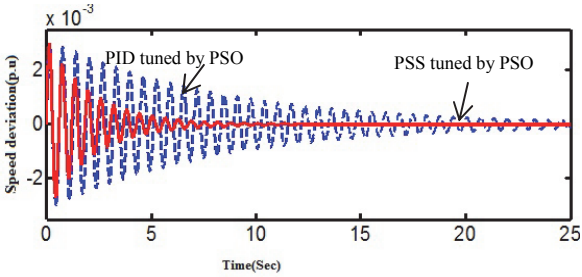

Fig. 10 – *Speed deviation of generator in the presence of SOFC in scenarios 1 and 2.*

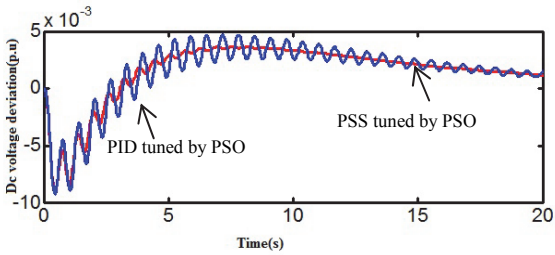

Fig. 11 – *DC voltage deviation of DC-DC converter in scenarios 1 and 2.*

4.1.3 Scenario 3

In this case, generator is equipped with PID controller that tuned by Multi-objective PSO. The convergence rate for two objective functions is shown in Fig. 12a. The speed deviation of the system with different controllers is shown in Fig. 13. As shown, the PID can stable the system. It can seen the speed deviation with PID tuned by MOPSO is better than that tuned with PSO with

less settling time and overshoot. Also, the DC voltage deviation of output DC-DC converter with different controllers are shown in Fig. 14.

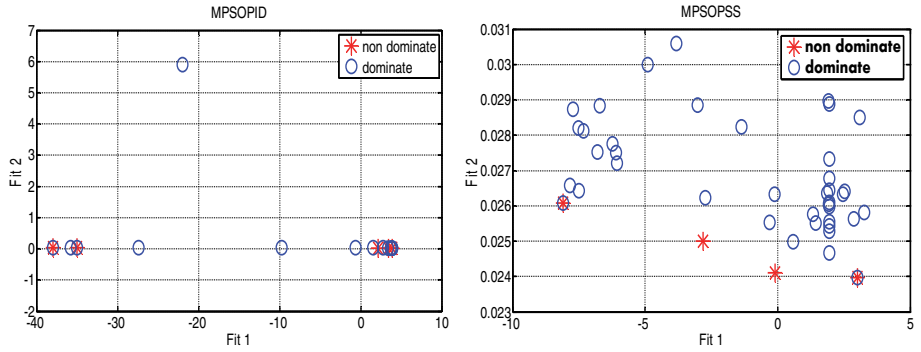

(a) (b)

Fig. 12 – *Variations of objective functions in scenarios 3 and 4.*

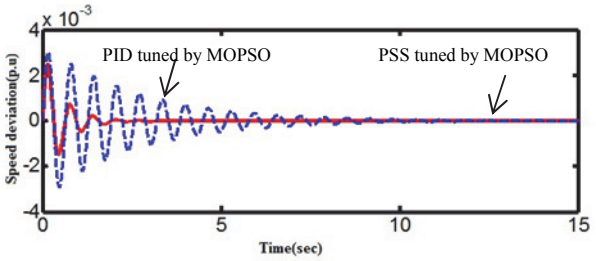

Fig. 13 – *Speed deviation in scenarios 3 and 4.*

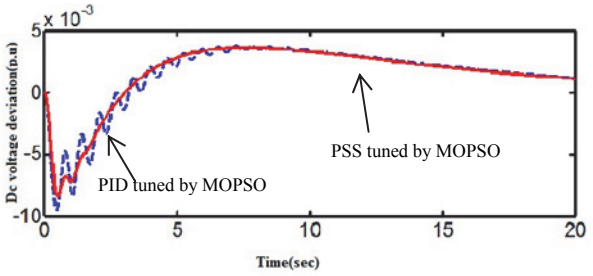

Fig. 14 – *DC voltage deviation of DC-DC converter in scenarios 3 and 4.*

4.1.4 Scenario 4

In this scenario, generator is equipped with a classic PSS that tuned by Multi-objective PSO. The convergence rate for two objective functions is shown in Fig. 12b. The performance of the PSS tuned based on the multiobjective function is compared to that of the PSS tuned using the single

objective functions as shown in Figs. 13 and 10, it can be seen that the speed deviation with MOPSO based PSS is better than that with PSO based PSS with less settling time and overshoot. Also, the DC voltage deviation of output DC-DC converter with different controllers is shown in Fig. 14.

4.2 A multi-machine connected to the SOFC

To assess the effectiveness and robustness of the proposed method over the other systems, the three-machine ten-bus power system, shown in Fig. 15, is considered. Details of the system data are given in [2]. The capacity of the SOFC power plant is assumed to be comparable to that of the synchronous generators in the case study. In this section, we have used the MOPSO technique as an effective algorithm, to tune the PSSs parameters and improve the small signal stability of the system.

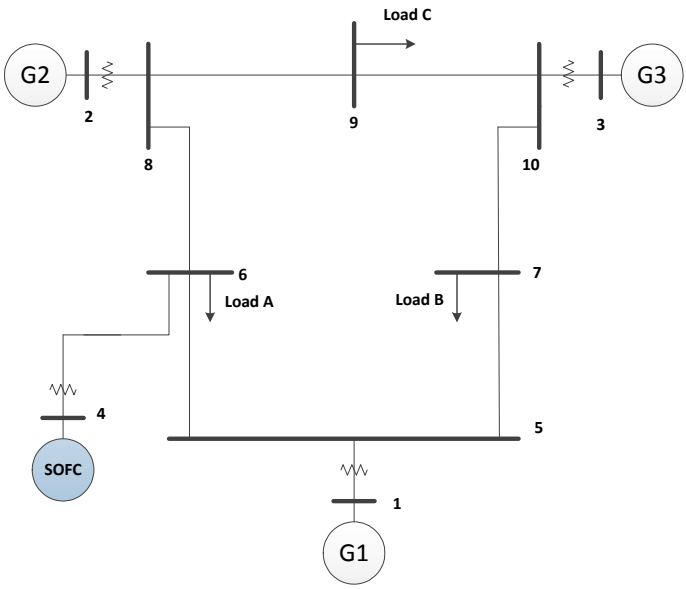

Fig. 15 – *Three-machine ten-bus system joint with SOFC power plant.*

4.2.1 Optimal tuning of PSSs parameters

The conventional structure of the PSS is used to reduce the system oscillations. In this study, PSS is connected to all the machines. In the provided method, we should set out the PSSs parameter, optimally to improve the system dynamic stability. The parameters of PSS (T_1, T_2, K_C) for all machines should be tuned by MOPSO and PSO algorithm. Typical ranges of the optimized parameters are [0.1 – 50] for K_C and [0.01 – 2] for T_1 and T_2. The optimized solutions are shown in **Table 3**.

The objective functions are the same objective functions at previous sections. The design problem can be formulated as the following constrained optimization problem, where the constraints are the stabilizers parameter bounds:

$$\begin{aligned} K_C^{\min} \le K_C \le K_C^{\max}, \\ T_1^{\min} \le T_1 \le T_1^{\max}, \\ T_2^{\min} \le T_2 \le T_2^{\max}. \end{aligned} \tag{45}$$

Table 3

The optimal solutions of power system stabilizers.

Parameters	G_1			G_2			G_3		
	T_1	T_2	K_C	T_1	T_2	K_C	T_1	T_2	K_C
Optimal value with PSO	1.019	0.11	10.4	1.05	0.03	23	1.9	0.01	15
Optimal value with MOPSO	1.81	0.04	42	1.09	0.65	35	0.93	0.05	10

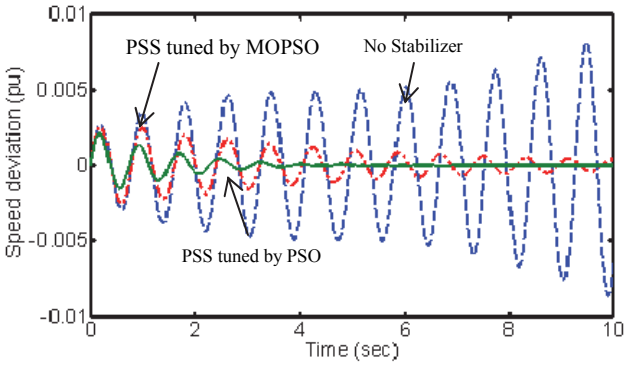

Fig. 16 – *Speed deviation between generator G1 and G2 with and without stabilizer.*

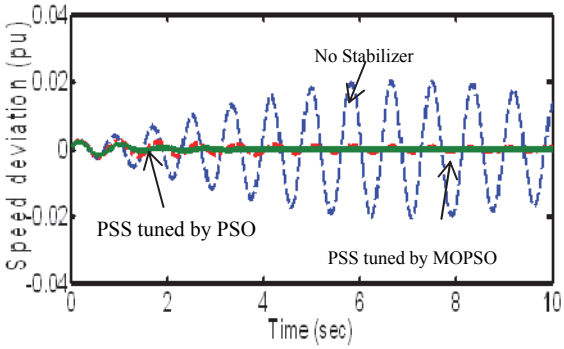

Fig. 17 – *Speed deviation between generator G1 and G3 with and without stabilizer.*

4.2.2 Time domain analysis

In this section, the performance of the proposed optimized PSS under transient conditions is verified by applying a step input signal. The system responses to this fault are shown in Figs. 16 and 17. In this case, the SOFC power generation is lower than the active power supply from the generators in the grid. Without installing any PSS, the oscillations cannot be damped because the system exhibits two modes of oscillation in this case: one unstable inter-area mode and one stable mode. Therefore, the SOFC power generation can makes instability in the system. The conventional PSSs are installed on the all synchronous generators and these parameters are tuned using the PSO and MOPSO algorithms. It can be seen that installing properly PSSs tuned by MOPSO on generators has the largest effect on the damping of the inter area oscillation mode. The speed deviation between generator G1 and G2 is shown in Fig 16. Fig. 17 shows the speed deviation between generator G1 and G3.

7 Conclusion

This paper shows the result of the power system joined to the SOFC unit on small signal stability and effect of the optimal stabilizers to reduce the low frequency oscillations. A PSS tuned by MOPSO is proposed for attenuate the low frequency oscillations of imported disturbance in power system in presence of a SOFC power generation. The optimization of parameters the CPSS and PID controller is carried out. To acquire the optimized parameters, the MOPSO algorithm is applied to solve the design problem. Simulation study in the SMIB connected to the SOFC power generation confirms that the stabilizing consequence of the proposed MOPSO based CPSS are much superior to those of the conventional and PID controller. It is concluded that the PSSs tuned using the multiobjective function achieves good robust and provides superior damping in comparison with the case when the single objective is used.

8 Appendix

Data for the single machine infinite bus is [19]:

– Transmission line:

$x_{ts} = 0.3\,p.u.,\quad x_{sb1} = 0.4\,p.u.,\quad x_{sb2} = 0.4\,p.u.,\quad x_s = 0.3\,p.u.$

– Generator:

$x_d = 1.3\,p.u.,\quad x_q = 0.47\,p.u.,\quad x_d^{'} = 0.3\,p.u.,\quad M = 7.4\,s,\quad D = 4\ p.u.,$

$T'_{d0} = 5\,\mathrm{s}$.

– AVR:

$T_A = 0.1\,s,\quad K_A = 10\,p.u.$

– Initial condition:

$V_{t0} = 1.0\,p.u.$, $V_{s0} = 1.0\,p.u.$, $V_{b0} = 1.0\,p.u.$, $V_{dc0} = 1.0\,p.u.$

– Parameters of the SOFC

$T = 1273°K$, $F = 96487$, $K_r = 0.966e-6\ mol/(s.A)$,

$R = 8.314$, $E_0 = 1.18V$, $U_{\max} = 0.9$, $U_{\min} = 0.8$ $U_{opt} = 0.85$,

$K_{h2} = 5.43e-4\,mol/(s.atm)$, $K_{o2} = 2.52e-3\ mol/(s.atm)$,

$t_{h2} = 26.1s$, $t_{h2o} = 78.3s$, $K_{h2o} = 2.81e-4\,mol/(s.atm)$, $T_f = 5s$,

$T_e = 0.08s$, $r_{ho} = 0.8$, $N_0 = 384$, $t_{o2} = 2.91s$, $r = 0.126\,\Omega$.

9 References

[1] J. Larminie, A. Dicks: Fuel Cell Systems Explained, J. Wiley & Sons, Chichester, 2003.

[2] M. Farooque, H.C. Maru: Fuel Cells-The Clean And Efficient Power Generators, Proceedings of the IEEE, Vol. 89, No. 12, 2001, pp. 1819 – 1829.

[3] Fuel Cell Technology Handbook, Edited by G. Hoogers, CRC press, Boca Raton, FL, 2002.

[4] P. Thounthong, B. Davat, S. Rael, P. Sethakul: Fuel Cell High-Power Applications, IEEE Industrial Electronics Magazine, Vol. 3, No. 1, 2009, pp. 32 – 46.

[5] Y.H. Li, S. Rajakaruna, S. S. Choi: Control of a Solid Oxide Fuel Cell Power Plant in a Grid-Connected System, IEEE Transactions on Energy Conversion, Vol. 22, No. 2, 2007, pp. 405 – 413.

[6] J. Padullesa, G. W. Aultb, J. R. McDonald: An Integrated SOFC Plant Dynamic Model for Power Systems Simulation, Journal of Power Sources, Vol. 86, No. 1–2, 2000, pp. 495 – 500.

[7] Y. Zhu, K. Tomsovic: Development of Models for Analyzing the Load-Following Performance of Microturbines and Fuel Cells, Electric Power Systems Research, Vol. 62, No. 1, 2002, pp. 1 – 11.

[8] D. Georgakis, S. Papathanassiou, S. Manias: Modeling and Control of a Small Scale Grid-Connected Pem Fuel Cell System, 36th Power Electronics Specialists Conference, Recife, Recife, Brazil, June 2005, pp. 1614 – 1620.

[9] K. Sedghisigarchi, A. Feliachi: Dynamic and Transient Analysis of Power Distribution Systems with Fuel Cells-Part I: Fuel-Cell Dynamic Model, IEEE Transactions on Energy Conversion, Vol. 19, No. 2, 2004, pp. 423 – 428.

[10] K. Sedghisigarchi, A. Feliachi: Dynamic and Transient Analysis of Power Distribution Systems with Fuel Cells-Part II: Control and Stability Enhancement, IEEE Transactions on Energy Conversion, Vol. 19, No. 2, 2004, pp. 429 – 434.

[11] S. Das, D. Das, A. Patra: Operation of Solid Oxide Fuel Cell based Distributed Generation. 4th International Conference on Advances in Energy Research 2013 (ICAER 2013), Energy Procedia, Vol. 54, 2014, pp. 439 – 447.

[12] E. M. Fleming, I. A. Hiskens: Dynamics of a Microgrid Supplied by Solid Oxide Fuel Cells, IREP Symposium, Bulk Power System Dynamics and Control-VII, Revitalizing Operational Reliability, Charleston, South Carolina, USA, 19 – 24 August, 2007, pp. 1 – 10.

[13] H. Wang, G. Li: Dynamic Performance of Microturbine and Fuel Cell in a Microgrid, International Conference on Mechatronic Science, Electric Engineering and Computer (MEC), Jilin, China, 19 – 22 August 2011, pp. 122 – 125.

[14] C. J. Hatziadoniu, A. A. Lobo, F. Pourboghrat, M. Daneshdoost: A Simplified Dynamic Model of Grid-Connected Fuel-Cell Generators, IEEE Transactions on Power Delivery, Vol. 17, No. 2, 2002, pp. 467 – 473.

[15] W. Du, H. F. Wang, X. F. Zhang, L. Y. Xiao: Effect of Grid-Connected Solid Oxide Fuel Cell Power Generation on Power Systems Small-Signal Stability, IET Renewable Power Generation, Vol. 6, No. 1, 2012, pp. 24 – 37.

[16] A. M. El-Zonkoly, A. A. Khalil, N. M. Ahmied: Optimal Tunning of Lead-Lag and Fuzzy Logic Power System Stabilizers Using Particle Swarm Optimization, Expert Systems with Applications, Vol. 36, No. 2, 2009, pp. 2097 – 2106.

[17] Y. H. Li, S. Rajakaruna, S. S. Choi: Control of a Solid Oxide Fuel Cell Power Plant in a Grid-Connected System", IEEE Transactions Energy Conversion, Vol. 22, No. 2, 2007, pp. 405 – 413.

[18] Y. N. Yu: Electric Power System Dynamics, Academic Press, Inc., New York, NY 10003, 1983.

[19] H. Shahsavari, A. Safari: Optimal Design of Novel Flpss for Power Network Connected Solid Oxide Fuel Cell Using of HSS Algorithm, International Journal of Energy and Statistics, Vol. 5, No. 2, 2017, p. 1750008.

[20] Modeling of Power Electronics Equipment (FACTS) in Load Flow and Stability Programs: A Representation Guide for Power System Planning and Analysis, Technical Brochure, CIGRE, 1999.

[21] J. Kennedy, R. Eberhart: Particle Swarm Optimization, Proceedings of IEEE International Conference on Neural Networks, Perth, WA, Australia, 27 November – 1 December 1995, pp. 1942 – 1948.

[22] A. Jalilvand, A. Safari, R. Aghmasheh: Design of State Feedback Stabilizer for Multimachine Power System Using PSO Algorithm, Pro IEEE International Multitopic Conference, INMIC 2008, Karachi, Pakistan, 23 – 24 December 2008, pp. 17 – 23.

[23] M. Rahmati, R. Effatnejad, A. Safari: Comprehensive Learning Particle Swarm Optimization (CLPSO) for Multi-objective Optimal Power Flow, Indian Journal of Science and Technology, Vol. 7, No. 3, 2014, pp. 262 – 270.

[24] A. Safari, N. Rezaei: Towards an Extended Power System Stability: An Optimized GCSC-Based Inter-Area Damping Controller Proposal, International Journal of Electrical Power and Energy Systems, Vol. 56, 2014, pp. 316 – 324.